

Lissajous Curve Methods for the Identification of Nonlinear Circuits: Calculation of a Physical Consistent Reactive Power

Tianqi Hong, *Student Member, IEEE*, and Francisco de León, *Fellow, IEEE*

Abstract—This paper presents a novel analysis of nonlinear circuits useful for the computation of the reactive power from only terminal measurements. The method computes the reactive power of unknown circuits based on the physical understanding of Maxwell equations. The proposed method is able to identify instantaneous quantities (circuit parameters, powers, etc.) for two physical equivalent models: series and parallel circuits. The parallel equivalent model shows advantages for multi-subsystems. Several numerical examples are provided for validation of the proposed method and to illustrate step-by-step the calculation details. To be compatible with digital instrumentation, a time discrete formulation is used for all calculations. All examples are simulated in MATLAB and the EMTP (Electro-Magnetic Transients Program).

Index Terms—Nonlinear circuits, nonsinusoidal excitation, power definitions, power flow, reactive power.

I. INTRODUCTION

STEINMETZ established alternating-current circuit theory in the last few years of the ninetieth century [1]. However, after more than a century, the definition of reactive power is still ambiguous for nonlinear circuits. According to the IEEE standard 1459–2010 [2], there is not yet available a power theory that can provide a common base for billing, power quality, and detection and mitigation of waveform distortion.

In the 1930s, Budeanu and Fryze developed power theories for nonsinusoidal excitations; see [3]. Budeanu proposed the concept of *distortion power* and Fryze started the concept of *instantaneous power decomposition*. After decades, Budeanu's theory was considered to be a misconception and Fryze's theory was further developed by Czarnecki. Based on the decomposition concept, Czarnecki developed the Currents' Physical Components (CPCs) method for both single-phase and three phase systems [4], [5]. However, although the CPCs are useful for engineering purposes, the mathematical decomposition lacks full physical existence and has been questioned by other researchers [6], [7].

Physical definitions of power quantities have been recognized by Emanuel in [8], which are based on the Poynting Vector (PV). The practical value of PV was disputed by Czarnecki [10]. In 2007, new power quantities derived from PV were defined by Sutherland [9]. In 2010 and 2012, a novel identification method for series nonlinear $R - L$ models was obtained from

the Poynting Vector Theorem (PVT) [11], [12]. Although this identification method can properly characterize series nonlinear systems, bringing physicality back to power theory, the instantaneous reactive power computed from this method does not properly add for multi-branch circuits.

This paper proposes an analytical tool with graphical representation (based on Lissajous curves) to analyze the energy (or power) flow at the PCC (point of common coupling) of an unknown nonlinear single-phase circuit. With this tool, one is able to identify the parameters (R , L , and C) of the unknown circuit using solely measurements of the instantaneous voltage and current at the PCC. In general R , L , and C are nonlinear or time varying and can be computed with very simple formulae. Once the circuit components are identified, physically correct power quantities can be obtained from first electromagnetic principles.

The contribution of this paper can also be seen as the generalization of the Fryze-Czarnecki theory for the modeling of active and reactive powers with time-varying circuit elements that have full physical meaning in terms of Maxwell equations. Four examples are provided to illustrate the proposed method. One can see that the method is accurate and the obtained circuit parameters have full physical meaning.

The paper is organized as follows: Section II describes the proposed definition of reactive power. Section III presents the Lissajous curve methods used for the identification of equivalent circuit elements for linear and nonlinear circuits. Section IV shows application examples and Section V summarizes the most important conclusions of the paper.

II. DEFINITION OF ACTIVE AND REACTIVE POWERS

All discussions in this paper are based on Maxwell's physical definitions of powers. The general expression coming from the Poynting Vector Theorem (PVT) describing the power transfer phenomena between a source and a load is:

$$\oint_{\mathcal{S}} \mathbf{E} \times \mathbf{H} \cdot d\mathcal{S} = - \int_{\mathcal{V}} \mathbf{E} \cdot \mathbf{J} d\mathcal{V} - \frac{\partial}{\partial t} \int_{\mathcal{V}} \left(\frac{\mathbf{H} \cdot \mathbf{B}}{2} + \frac{\mathbf{E} \cdot \mathbf{D}}{2} \right) d\mathcal{V}, \quad (1)$$

where \mathbf{E} is the electric-field vector in V/m, and \mathbf{H} is the magnetic field intensity vector in A/m, \mathbf{J} is the current density vector in A/m², \mathbf{B} is the magnetic flux density vector in T, \mathbf{D} is the electric displacement field vector in C/m², \mathcal{S} refers to a closed surface, and \mathcal{V} refers to the volume enclosed by \mathcal{S} .

According to (1), the transferred energy is split into two parts (and only two parts): the power of consumed energy is the active power; and the power of stored and restored energy in electric and magnetic fields is the reactive power. Mathematically, we have:

$$a(t) = \text{instantaneous active power} = - \int_{\mathcal{V}} \mathbf{E} \cdot \mathbf{J} d\mathcal{V} \quad (2)$$

$$r(t) = \text{instantaneous reactive power}$$

Manuscript received May 01, 2015; revised August 03, 2015; accepted October 10, 2015. Date of publication November 20, 2015; date of current version December 04, 2015. This paper was recommended by Associate Editor C. Fernando.

The authors are with the Department of Electrical and Computer Engineering, New York University, Brooklyn, NY, 11201 USA (e-mail: th1275@nyu.edu; fdeleon@nyu.edu).

Color versions of one or more of the figures in this paper are available online at <http://ieeexplore.ieee.org>.

Digital Object Identifier 10.1109/TCSI.2015.2495780

$$= - \frac{\partial}{\partial t} \int_{\mathcal{V}} \left(\frac{H \cdot B}{2} + \frac{E \cdot D}{2} \right) d\mathcal{V}. \quad (3)$$

Based on Maxwell's electromagnetic theory, the reactive power only exists when the system has elements capable of storing energy. Note that today a gamut of reactive power definitions can be found in the literature. Most of them express that reactive power can exist in resistive loads (lacking energy storage elements) when fed from nonlinear sources; see [13] as an example. The problem with these calculations is the use of non-physical definitions for the calculation of reactive power. This paper proposes that the only physically correct reactive power should be consistent with (3). In the rest of this paper, the Maxwell reactive power defined in (3) is called the *instantaneous reactive power*.

The physical (in Maxwell terms) definitions of active and reactive powers proposed in this section assume the knowledge of the instantaneous equivalent resistance $R(t)$, inductance $L(t)$, and capacitance $C(t)$.

According to the physical definition, the instantaneous Joule power $a_J(t)$ is defined as the power consumed by the resistance and given by:

$$a_J(t) = v_R(t)i_R(t) = R(t)i_R^2(t), \quad (4)$$

where $v_R(t)$ and $i_R(t)$ are the voltage and current of $R(t)$. The instantaneous power in an inductor $r_L(t)$ is defined as the time derivative of the energy stored in the inductor given by:

$$r_L(t) = \frac{d}{dt} \left(\frac{1}{2} L(t) i_L^2(t) \right) = \frac{dL(t)}{2dt} i_L^2(t) + i_L(t) \frac{di_L(t)}{dt} \quad (5)$$

where $i_L(t)$ is the current in the equivalent inductor. For a constant inductor L , we have:

$$r_L(t) = i_L(t) \frac{di_L(t)}{dt} L = \frac{1}{L} v_L(t) \int v_L(t) dt = v_L(t) i_L(t) \quad (6)$$

where $v_L(t)$ is the voltage across the equivalent inductor. For clear illustration, the integral of voltage (units of magnetic flux) is denoted as:

$$\phi(t) = \int v(t) dt. \quad (7)$$

When there is no flux in the circuit, $\phi(t)$ can be treated as a mathematical function of voltage which can always be computed from terminal measurements. In most nonlinear circuits, the integral of voltage is not the flux in the model inductor.

The instantaneous power $r_C(t)$ in a capacitor is computed from the time derivative of the energy stored as follows:

$$r_C(t) = \frac{d}{dt} \left(\frac{C(t) V_C^2(t)}{2} \right) = \frac{dC(t)}{2dt} v_C^2(t) + v_C(t) \frac{dv_C(t)}{dt} C(t) \quad (8)$$

where $v_C(t)$ is the voltage across the equivalent capacitor $C(t)$. For a constant capacitor C , we have:

$$r_C(t) = v_C \frac{dv_C(t)}{dt} C = \frac{1}{C} i_C(t) \int i_C(t) dt = v_C(t) i_C(t) \quad (9)$$

where $i_C(t)$ is the current of the equivalent capacitor C .

In a general system, $r_L(t)$ and $r_C(t)$ may not be the instantaneous reactive power $r(t)$, because of hysteresis power $a_H(t)$ or nonlinear power $a_N(t)$ caused by connecting and disconnecting energy store-able elements by a switch (see example in Section IV-C). Note that $a_N(t)$ and $a_H(t)$ exist in both capacitors and inductors. Hence, the instantaneous active power $a(t)$ which is defined as the power consumed in the system is expressed as:

$$a(t) = a_J(t) + a_H(t) + a_N(t). \quad (10)$$

The instantaneous active power of a nonlinear general system is almost impossible to obtain because it is difficult to calculate

the instantaneous hysteresis power and nonlinear power from only terminal measurements. However, it is possible to obtain the average hysteresis power P_H and nonlinear power P_N .

According to the definition of instantaneous active power, the average active power P_a of one period T (of the fundamental component) is defined as:

$$P_a = \frac{1}{T} \int_0^T a(t) dt = \frac{1}{T} \int_0^T |a(t)| dt. \quad (11)$$

Note that for a passive circuit $a(t) \geq 0$ and thus one can substitute $a(t)$ by $|a(t)|$ in (11) to get a similar expression as for reactive power (see below). Based on the principle of conservation of energy, the average active power P_a should equal the power consumed by the circuit P_C . Hence, we have:

$$P_a = P_C = \frac{1}{T} \int_0^T v(t)i(t) dt. \quad (12)$$

Due to the nonlinearity and non-ideality of general circuit elements, the following relationship exists:

$$r_{nz}(t) = r_L(t) + r_C(t) = r(t) + a_H(t) + a_N(t), \quad (13)$$

where $r(t)$ is the instantaneous reactive power and $r_{nz}(t)$ is the total instantaneous power of energy store-able elements (which may include losses or energy not restored to the source). Since $r(t)$ is defined as a quantity to evaluate the speed of the energy store/restore process between the reactive circuit elements and the source, the integral of $r(t)$ over a period should equal to zero. Thus $|r(t)|$ is used to compute the reactive power.

Since (13) takes into consideration that inductors and capacitors may be lossy, it is possible that the average of $r_L(t)$ and/or $r_C(t)$ is not equal to zero. This non-zero (active) power P_{nz} is calculated as:

$$\begin{aligned} P_{nz} &= P_H + P_N = \frac{1}{T} \int_0^T [a_H(t) + a_N(t)] dt \\ &= \frac{1}{T} \int_0^T [r_L(t) + r_C(t)] dt \end{aligned} \quad (14)$$

where P_N is the average nonlinear power and P_H is the average hysteresis power. P_{nz} is the power consumed by nonlinear inductors and/or capacitors.

Hence, instead of computing average active power P_a from (11), we calculate it as:

$$P_a = P_J + P_H + P_N = P_J + P_{nz} \quad (15)$$

where P_J is the average joule power.

To compute Q (the average reactive power, say the power that can be compensated with reactive elements) corresponding to actual reactive power $r(t)$, several methods are considered:

- 1) The "textbook" approach is to use the amplitude of the instantaneous reactive power for linear circuits. The authors have reviewed over 100 circuit theory books and found that the most common mathematical expression for reactive power of linear circuits is [14]:

$$Q_{\text{textbook}} = \max \{r(t)\} = \frac{V_m I_m}{2} \sin(\theta_v - \theta_i) \quad (16)$$

where V_m and I_m are the amplitude of the voltage and current at the terminal measurements (PCC) of Fig. 1, respectively; θ_v is the angle of the fundamental frequency component of voltage and θ_i is the angle of the fundamental frequency component of current.

- 2) The IEEE Std. 1459 [2] definition of reactive power for linear and nonlinear circuits is:

$$Q_{1459} = \frac{\omega_1}{kT} \int_{t_0}^{t_0+kT} i_1(t) \left[\int_{t_0}^t v_1(\tau) d\tau \right] dt \quad (17)$$

where ω_1 , $v_1(t)$, and $i_1(t)$ are the fundamental frequency components of the terminal measurements in Fig. 1 obtained from Fourier analysis and k is an integer representing the number of cycles used in the calculation.

- 3) A full physical alternative to compute the reactive power over a period, proposed here, is to take the average of the absolute instantaneous reactive power expressed as follows:

$$Q_{physical} = \frac{\pi}{2T} \int_0^T |r(t)| dt = \frac{\pi}{2T} \left[\int_0^T |r_{nz}(t)| dt - TP_{nz} \right]. \quad (18)$$

A factor $\pi/2$ is introduced in (18) to numerically match with $Q_{textbook}$ and Q_{1459} for linear circuits. In (17) the IEEE standard added ω_1 for the same purpose. The term $\int_0^T |r(t)| dt$ is the total energy stored/restored between inductive and capacitive elements and the source during a period. $\int_0^T |r_{nz}(t)| dt$ is the total energy stored/restored, but it includes energy that is not returned to the source (losses or consumed elsewhere in the circuit). TP_{nz} is the energy that failed to be restored to source, which is computed from (14). Note that $|r(t)|$ is not instantaneously equal to $|r_{nz}(t)| - |a_H(t) + a_N(t)|$. We state that the following integral (without $\pi/2$):

$$Q_{average} = \frac{1}{T} \int_0^T |r(t)| dt \quad (19)$$

is truly the average reactive power and perhaps should have been used from the beginning (since this is the definition coherent with Maxwell equations). At this time in history, it is perhaps too late to remove the historical factors from the calculation of Q .

III. LISSAJOUS CURVES FOR THE IDENTIFICATION OF EQUIVALENT CIRCUIT ELEMENTS

A. Series and Parallel Equivalent Circuits

From only terminal measurements of instantaneous voltage and current, it is impossible to obtain the detailed internal connectivity and value of every parameter of a general circuit. To analyze the energy (or power) flow at the point of common coupling (PCC) of an unknown system, some assumptions are needed. In this paper, an arbitrary system is represented as one of two types of circuits. The series model consists of a nonlinear resistor in series with a nonlinear element able to store energy. The other one, the parallel model, contains a nonlinear resistor connected in parallel with a nonlinear element that is able to store energy; see Fig. 1.

According to Joule's law, the instantaneous power in the resistors of the series and parallel models are, respectively:

$$a_{Rs}(t) = v_R(t)i(t) = R_s(t)i^2(t) \quad (20a)$$

$$a_{Rp}(t) = v(t)i_R(t) = \frac{v^2(t)}{R_p(t)} \quad (20b)$$

where $v(t)$ and $i(t)$ are the measured voltage and current at the PCC, $v_R(t)$ and $i_R(t)$ are the voltage and current of the resistor, $a_{Rs}(t)$ is the power of the resistor in the series model, and $a_{Rp}(t)$ is the power in the resistor of the parallel model. Based on Kirchhoff's Voltage Law (KVL) and Kirchhoff's Current Law (KCL),

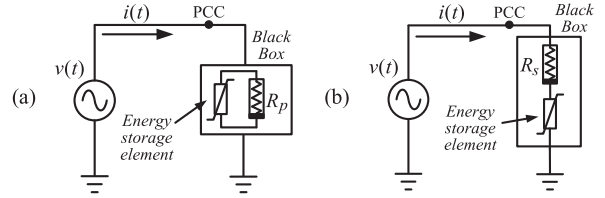


Fig. 1. Two energy equivalent models for the analysis of arbitrary electrical circuits: (a) parallel model; (b) series model.

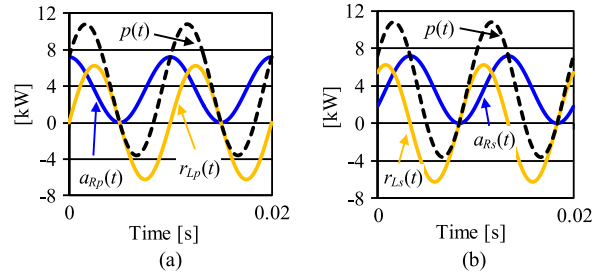


Fig. 2. Instantaneous powers of the two equivalent models, $a_R(t)$ is the power of the resistive element, $r_L(t)$ is the power of the inductive element, $p(t) = a_R(t) + r_L(t)$ is the instantaneous power at the PCC: (a) parallel model; (b) series model.

one can compute the instantaneous power of the energy storage element (by subtraction) as follows:

$$\begin{aligned} r_{Es}(t) &= v_E(t)i(t) = (v(t) - v_R(t))i(t) \\ &= v(t)i(t) - a_{Rs}(t) \end{aligned} \quad (21a)$$

$$\begin{aligned} r_{Ep}(t) &= v(t)i_E(t) = v(t)(i(t) - i_R(t)) \\ &= v(t)i(t) - a_{Rp}(t) \end{aligned} \quad (21b)$$

where $r_{Es}(t)$ is the power in the storage element of the series model and $r_{Ep}(t)$ is the power in the storage element in the parallel model, $v_E(t)$ and $i_E(t)$ are the voltage and current of the energy storage element. Therefore, to compute equivalent circuits with the same energy properties only parameters $R_s(t)$ and $R_p(t)$ need to be identified. This is different from the formulations of Fryze and Czarnecki [3], [4] where a constant conductance is computed.

To illustrate the parameter identification process and the differences between the series and parallel equivalent circuits, consider an unknown linear system, whose terminal measurements are (note that the current is lagging the voltage):

$$v(t) = 120\sqrt{2} \cos 100\pi t \quad [\text{V}] \quad (22)$$

$$i(t) = \frac{120}{\sqrt{2}} \cos \left(100\pi t - \frac{\pi}{6} \right) \quad [\text{A}]. \quad (23)$$

For each of the equivalent circuits the instantaneous power at the PCC, $p(t) = v(t)i(t)$, can be decomposed into two powers: the power consumed in the resistor $a_R(t)$ and the power stored in the inductor $r_L(t)$. These powers are different in each equivalent circuit; see Fig. 2. In a linear case, as the one illustrated here, only the phase of the sine functions is different between the series and parallel circuits (note that $r(t) = r_L(t)$ in this case because the inductor has no losses). The average and peak values of instantaneous active and reactive powers are identical, which points to systems with the same P and Q regardless of its connectivity. Note that $p(t)$ is the starting point of the decomposition process and therefore it is always the same for a linear or nonlinear circuit (series or parallel).

In a nonlinear system, the average of the active power is the same for both models. However, the average and peak of the instantaneous reactive powers are different. Finding a proper

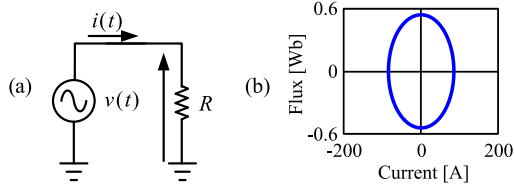


Fig. 3. Sinusoidal source feeding a linear resistor: (a) electrical circuit; (b) $\phi - i$ Lissajous curve.

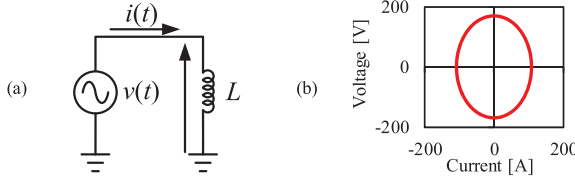


Fig. 4. Sinusoidal source feeding a linear inductor: (a) electrical circuit; (b) $v - i$ Lissajous curve.

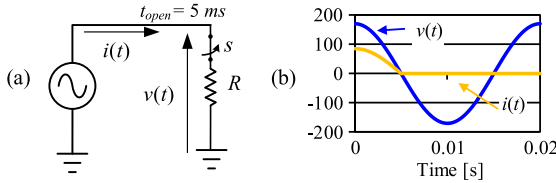


Fig. 5. Sinusoidal source feeding a linear resistor with a switch: (a) electrical circuit; (b) voltage $v(t)$ and current $i(t)$ of source.

method to evaluate the reactive power in a general system is important for completing the power theory. The following subsections establish a novel tool for the analysis of an unknown nonlinear system and for the computation of powers based on the two models (series and parallel). For a circuit fed from a sinusoidal excitation, capacitors can be mapped one-to-one to negative inductors [11]; therefore only two elements (a resistor and an inductor) need to be identified. Hence, we start our discussion with sinusoidal excitation, but nonsinusoidal excitation is discussed in Section III-D.

B. 3-D Lissajous Curves

Measurements of the instantaneous voltage (v) and current (i) of the system at the PCC can always be obtained. To explain 3-D Lissajous curves, two possible 2-D Lissajous curves for a given circuit are obtained first: voltage versus current ($v - i$); and voltage integral (or flux ϕ) versus current ($\phi - i$).

Due to the simplicity of a linear circuit, 2-D Lissajous curves can be used for the analysis of the power at the PCC, where “ $v - i$ ” can be used to obtain the average reactive power (Q) and “ $\phi - i$ ” can be used to calculate the average active power (P).

Consider a resistive load ($R = 2 \Omega$) fed from a 50 Hz sinusoidal voltage source as shown in Fig. 3(a). The instantaneous voltage, current, and flux (or voltage integral) are:

$$v(t) = 120\sqrt{2} \cos(100\pi t) \quad [\text{V}] \quad (24)$$

$$i(t) = 84.85 \cos(100\pi t) \quad [\text{A}] \quad (25)$$

$$\phi(t) = \int_0^T v(\tau) d\tau = 0.54 \sin(100\pi t) \quad [\text{Wb}]. \quad (26)$$

The (active) average power consumed in this circuit is computed from:

$$P_C = \frac{1}{T} \int_0^T v(t)i(t)dt = \frac{1}{2}RI_m^2 = 7.2 \text{ [kW]}. \quad (27)$$

The corresponding $\phi - i$ Lissajous curve is given in Fig. 3(b). One can appreciate that the curve describes an ellipse with horizontal and vertical maximum values of $I_m = 84.85 \text{ A}$ and $\Phi_m = 0.54 \text{ Wb}$, respectively. The area of the ellipse is the energy consumed by the resistor. Then, the active power can be computed as the average of the energy as follows:

$$P_a = \frac{1}{T}(\text{Area}) = \frac{1}{T} \int_0^T i(t)v(t)dt = 7.2 \text{ [kW]}. \quad (28)$$

For the inductive circuit ($L = 5 \text{ mH}$) fed by the same voltage source shown in Fig. 4(a), the instantaneous current is:

$$i(t) = 108.03 \sin(100\pi t) \quad [\text{A}] \quad (29)$$

and the reactive power can be obtained by substituting (24) and (29) into (16) as follows:

$$\begin{aligned} Q &= Q_{\text{textbook}} = \max \{v(t)i(t)\} = \frac{V_m I_m}{2} \sin(90^\circ) \\ &= 9.166 \text{ [kvar]}. \end{aligned} \quad (30)$$

The corresponding $v - i$ Lissajous curve is plotted in Fig. 4(b). Similarly to the resistive case, the reactive power (Q) of this circuit can be calculated from the area of the $v - i$ curve as follows [2]:

$$\begin{aligned} Q &= \frac{1}{\omega T}(\text{Area}) = \frac{1}{2\pi} \left| \int_{i(0)}^{i(T)} v(t)di(t) \right| \\ &= -\frac{V_m I_m}{\omega T} \int_0^T \cos \omega t d \sin \omega t = \frac{V_m I_m}{2T} T = 9.166 \text{ [kvar]}. \end{aligned} \quad (31)$$

Equation (31) is an expression used to compute the physical reactive power over a period, or a definition of Q , from the area of the $v - i$ Lissajous curve. Note that a division by ω is needed to make the value of (31) equal to the traditional reactive power definition. Equation (31) is used to illustrate that reactive power can be obtained from the area of the Lissajous curve for a linear circuit. However, for a general circuit, reactive power should be computed from (18).

We remark that 2-D Lissajous curves are not sufficient for the analysis of nonlinear circuits. Take for example the resistive nonlinear circuit ($R = 2 \Omega$) shown in Fig. 5(a), the controlled switch S is closed at $t = 0$ and opened at $t = 5 \text{ ms}$ (quarter of a cycle) periodically.

The corresponding $v - i$ Lissajous curve is plotted in Fig. 6(a). For a purely resistive load (R), voltage $v(t)$ and current $i(t)$ are in phase. Hence, a straight line with R as the slope can be seen at the beginning of the $v - i$ Lissajous curve (first quadrant). After one quarter cycle, when both voltage and current are zero, the switch S opens (Lissajous curve is at the origin). After this, the voltage $v(t)$ still exists but the current $i(t)$ is zero (the switch is considered to be a part of the load). As the time progresses, the $v - i$ Lissajous curve moves down and up along the voltage axis from zero to negative maximum and from negative maximum to positive maximum (as illustrated with the continuous arrows). At that last point $i(t)$ jumps from zero to its maximum value when the switch closes (following the dotted arrow) and a new cycle starts. The voltage integral $\phi(t)$ is 90° behind $i(t)$, hence the $\phi - i$ Lissajous curve can be drawn as in Fig. 6(b) following the same method. Note that it is not physically correct to have a non-zero reactive power in a resistive circuit since energy cannot be stored in a resistor. In contrast, the active power (P_a) can be calculated

correctly from the 2-D Lissajous curve of Fig. 6(b) using (28). The process is as follows (note that $i(t) = 0$ from $T/4$ to T):

$$\begin{aligned} P_a &= \frac{1}{T}(\text{Area}) = \frac{1}{T} \int_0^{\frac{T}{4}} i(t)v(t)dt = \frac{1}{T} V_m I_m \int_0^{\frac{T}{4}} \cos^2(\omega t) dt \\ &= \frac{V_m I_m}{2} \cdot \frac{1}{4} = \frac{84.85 \times 120\sqrt{2}}{8} = 1.8 \text{ [kW]}. \end{aligned}$$

Computing the reactive power by averaging the area under the curve (hatched area in Fig. 6(a)) of $v - i$ curve, we have:

$$\begin{aligned} Q &= \frac{(\text{Area})}{2\pi} = \frac{1}{2\pi} \left| \int_{i(0)}^{i(\frac{T}{4})} v(t) di(t) \right| \\ &= \frac{V_m I_m}{T} \left| \int_0^{\frac{T}{4}} \frac{\sin 2\omega t}{2} dt \right| = \frac{V_m I_m}{2\omega T} = 1.146 \text{ [kvar]} \neq 0. \end{aligned} \quad (32)$$

To analyze both linear and nonlinear systems, 3-D Lissajous Curves (3-D LCs) are introduced in this paper, which are the combination of two 2-D Lissajous curves. A 3-D Lissajous curve can be obtained by joining two 2-D Lissajous curves; see Fig. 7. Based on Figs. 6(a) and 6(b), the 3-D Lissajous curve of the nonlinear circuit (linear resistor with a switch) can be obtained. The projections of the curve over the $v - i$ and $\phi - i$ axes are the 2-D Lissajous curves described above.

Since there are two different models (series or parallel), 3-D Lissajous curves are separated into two different types. For the parallel models, the corresponding 3-D parallel Lissajous curves (3-D PLC) are plotted in coordinates consisting of voltage, voltage integral (flux ϕ), and current axes (parallel coordinate). Each instantaneous state of a given system can be described as a point $P_{pt}(v(t), \phi(t), i(t))$ in this 3-D PLC; subscript pt stands for parallel type.

For series models, the corresponding 3-D series Lissajous curves (3-D SLC) are drawn in coordinates of current, current derivative (DI), and voltage (series coordinate). Any point P_{st} of this 3-D SLC is presented as: $P_{st}(i(t), di(t)/dt, v(t))$; subscript st stands for series type.

Based on the principle of 3-D LCs, we postulate that each plane in the Lissajous coordinates (parallel or series) represents a two-element linear circuit with series or parallel connectivity. This postulate is proven for parallel model only, the same argument can be proven for the series model using a similar process. In the following proof, only inductive and resistive elements are considered since capacitors can be mapped to negative inductors under sinusoidal excitation; see Section III-D.

For two elements in a linear system with parallel connection see Fig. 1(a), we can write:

$$v(t) = R_p i_R(t), \quad (33)$$

$$\begin{aligned} \phi(t) &= \int_0^t v(\tau) d\tau = \int_0^t L_p \frac{di_L(\tau)}{d\tau} d\tau \\ &= \phi(0) + L_p (i_L(t) - i_L(0)), \end{aligned} \quad (34)$$

where $i_L(0)$ is the initial current of the inductance, $\phi(0)$ is the initial flux of the inductor, and L_p is the inductance of system. Assuming $i_L(0) = 0$ and $\phi(0) = 0$, and solving (33) and (34) for currents after applying KCL to the parallel circuit, we have:

$$i(t) = \frac{v(t)}{R_p} + \frac{\phi(t)}{L_p} \quad (35)$$

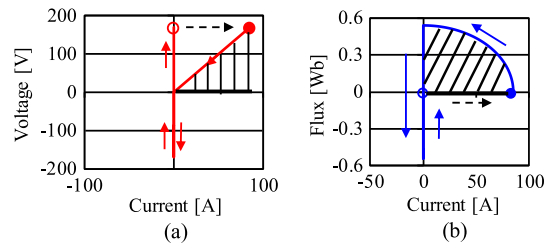


Fig. 6. 2-D Lissajous curves of sinusoidal source feeding a linear resistor with a switch: (a) $v - i$ Lissajous curve; (b) $\phi - i$ Lissajous curve.

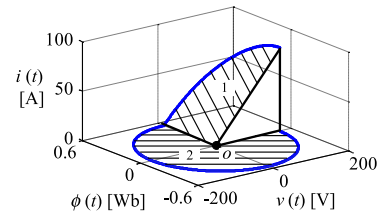


Fig. 7. 3-D Lissajous curve in parallel coordinate ($v(t)$, $\phi(t)$, $i(t)$).

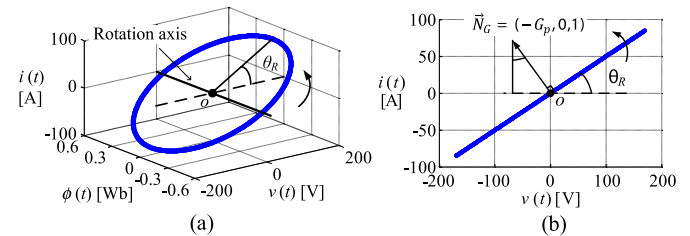


Fig. 8. 3-D and 2-D Lissajous curves for a constant resistive system under sinusoidal voltage excitation: (a) 3-D Lissajous curve; (b) 2-D $v - i$ Lissajous curve.

which represents a plane function in the parallel coordinate system. To avoid a numerical problem in the discussion below when R_p or L_p become infinity, (35) is rewritten as:

$$i(t) = G_p v(t) + \Gamma_p \phi(t), \quad (36)$$

where $G_p = R_p^{-1}$; $\Gamma_p = L_p^{-1}$. Note that G_p and Γ_p in general are functions of time, but they are constant in this (linear) example.

C. Calculation of the Parallel Model

According to (36), when $\Gamma_p = 0$, we have:

$$G_p(t) = \frac{i(t)}{v(t)} = \tan \theta_R, \quad (37)$$

where θ_R is shown in Fig. 8. Hence, the corresponding normal vector of a resistive plane can be written as: $\vec{N}_G = (v, \phi, i) = (-G_p, 0, 1)$. For a sinusoidal voltage source, the 3-D PLC of a resistive system is shown in Fig. 8(a). To illustrate the relationship in (37), the $v - i$ Lissajous curve is plotted in Fig. 8(b). According to (37) and Fig. 8(b), when G_p increases from zero to infinity, the resistive plane rotates around the flux ϕ axis from 0 to 90° . The Lissajous curve projection on the voltage plane is fixed by the amplitude of the voltage source. Similarly, when $G_p = 0$ we have:

$$\Gamma_p = \frac{i(t)}{\phi(t)} = \tan \theta_L, \quad (38)$$

where θ_L is shown in Fig. 9. Hence, a corresponding normal vector of an inductive plane is $\vec{N}_\Gamma = (v, \phi, i) = (0, \Gamma_p, 1)$. For a sinusoidal voltage source, the inductive 3-D PLC is shown in Fig. 9(a) and its corresponding 2-D Lissajous curve ($\phi - i$) is plotted in Fig. 9(b). According to (38) and Fig. 9(b), when Γ_p increases from zero to infinity, the pure inductive plane rotates around voltage v axis from 0 to 90° .

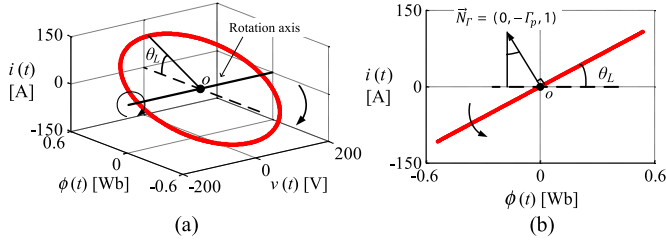


Fig. 9. 3-D and 2-D Lissajous curves of a constant inductive system under sinusoidal voltage excitation: (a) 3-D Lissajous curve; (b) 2-D Lissajous curve.

Remark that the normal vector of a plane is not unique. Hence, normal vector \vec{N}_G and normal vector \vec{N}_F are written as:

$$\vec{N}_G = (v, \phi, i) = (-N_v, 0, N_{iR}) \quad (39)$$

$$\vec{N}_F = (v, \phi, i) = (0, -N_\phi, N_{iL}) \quad (40)$$

where N_v is the amplitude of voltage component of normal vector \vec{N}_G in V, N_ϕ is the amplitude of flux component of \vec{N}_F in Wb, N_{iR} and N_{iL} are the current components of \vec{N}_G and \vec{N}_F in A.

Based on KCL, any two-element linear system with parallel connection is a combination of those two planes and the normal vector of that combined circuit plane \vec{N}_{CP} is:

$$\vec{N}_{CP} = \vec{N}_G + \vec{N}_F = (-N_v, -N_\phi, N_i) \quad (41)$$

where $N_i = N_{iR} + N_{iL}$. A plane can be defined by a normal vector and a known point on the plane. Assume that two known points in a plane are (v_0, ϕ_0, i_0) and (v, ϕ, i) . A vector between these two points can be obtained by subtracting the coordinates of the points as $\vec{l} = (v - v_0, \phi - \phi_0, i - i_0)$. The scalar product of this vector and a normal vector $\vec{N}_{CP} = (-N_v, -N_\phi, N_i)$ should be zero ($\vec{l} \cdot \vec{N}_{CP} = 0$). Hence, the function of the circuit plane can be written as:

$$N_v(v(t) - v_0) + N_\phi(\phi(t) - \phi_0) - N_i(i(t) - i_0) = 0. \quad (42)$$

By substituting three non-collinear points into (42), a normal vector can be obtained. Assuming that the origin is located at this circuit plane, mathematically expressed as:

$$N_v v_0 + N_\phi \phi_0 - N_i i_0 = 0, \quad (43)$$

one gets:

$$N_v v(t) + N_\phi \phi(t) - N_i i(t) = 0. \quad (44)$$

Because of the consistent relationship between a sinusoidal voltage and its integral, when the source voltage reaches its maximum value V_m , its integral ϕ is zero and the current is proportional to V_m . Replacing $v(t)$ and $\phi(t)$ and $i(t)$ in (44) by this steady relationship, we have:

$$N_v V_m + N_\phi \cdot 0 - N_i I = N_v V_m - N_i I_{Rm} = 0, \quad (45)$$

where I_{Rm} is the maximum value of the current in the resistive branch, and

$$G_p = \frac{I_{Rm}}{V_m} = \frac{N_v}{N_i}. \quad (46)$$

Following a similar approach, Γ_p can be computed as:

$$L_p^{-1} = \Gamma_p = \frac{I_{Lm}}{\phi_m} = \frac{N_\phi}{N_i}. \quad (47)$$

where I_{Lm} is the maximum value of the current in the inductor. The resistance and inductance of linear circuits with parallel connection can be computed with (46) and (47), respectively.

For nonlinear systems, we assume that any two-element system has a small period Δt where the resistance and inductance are constant. Based on this assumption, the 3-D Lissajous

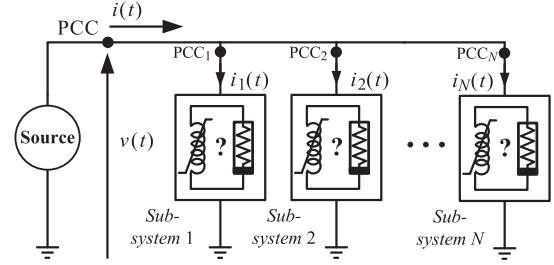


Fig. 10. Topology of a general multi-branch nonlinear system.

curve for a nonlinear system can be linearized using a piece-wise approximation. Each linearized section can be assigned to a corresponding circuit plane, which means two determined circuit parameters. By applying (46) and (47) to each linearized circuit plane, the time varying parallel model of the two-element nonlinear system can be obtained. The details of the computation process, including linear and nonlinear examples, are provided in Section IV below.

Given that the resistance can be computed as:

$$R(t) = \frac{v(t)}{i_R(t)}, \quad (48)$$

the resistor is a “memoryless” element (each point depends only on quantities at time t). In contrast, an inductor has “memory” since information from the past is needed; see (34). We calculate the instantaneous resistance using (46) and the current of the inductive branch can be computed from KCL as:

$$i_L(t) = i(t) - i_R(t) = i(t) - G_p(t)v(t). \quad (49)$$

According to the voltage-current relation of an inductance, the correct inductance can be obtained by:

$$L(t) = \frac{v(t)}{\frac{di_L(t)}{dt}}. \quad (50)$$

Remark that any hysteretic inductor can be made equivalent to a nonlinear resistor connected in parallel with a nonlinear inductor [12]; see Section IV-C. Based on the 3-D PLC method, the hysteresis power will be merged into the system equivalent resistor automatically. Now, we can compute the current in the resistive and inductive branches. With the current in each branch, the instantaneous power quantities can be computed from first electromagnetic principles using (20) and (21).

Based on the two-element parallel model, only two parameters (resistance and inductance) can be obtained. For an N -element system, only two equivalent parameters can be obtained from measurements at the PCC.

Because the branch voltage of a parallel circuit is the same and the currents must comply with KCL, for multi-branch systems as the one in Fig. 10, one expects the power quantities to fulfill the following properties:

$$P = \sum P_i; \quad Q = \sum Q_i \quad (51)$$

$$a(t) = \sum a_i(t); \quad r(t) = \sum r_i(t) \quad (52)$$

where P and Q are the average active and reactive powers of the entire system. P_i and Q_i are the average powers of branch i . $a(t)$ and $r(t)$ are the total instantaneous active and reactive powers and a_i and r_i are the instantaneous powers of branch i .

D. 4-D Lissajous Curve for Non-Sinusoidal Excitation

To fully analyze circuits under nonsinusoidal excitation a fourth axis needs to be added because inductors and capacitors no longer store/restore energy in phase with each other (see below). Thus one axis is used to compute the inductor and

another one needs to be added to compute the capacitor. It is not possible to provide a pictorial representation, but mathematically the concept of 4-D Lissajous curves is simply the addition of another hyperplane to the 3-D Lissajous curves.

According to [11], the relationship between the inductance and capacitance is:

$$C = \frac{1}{L} \frac{\int i(t) dt}{\frac{di(t)}{dt}} = \frac{1}{L} A(t). \quad (53)$$

The function $A(t)$ is constant under sinusoidal current excitation since the sine or cosine functions in the numerator and denominator cancel. For a constant capacitor C , the corresponding negative inductance is:

$$L = -\frac{1}{\omega^2 C}. \quad (54)$$

Under nonsinusoidal excitation, the poles and zeroes of $A(t)$ no longer occur at the same time t , therefore function $A(t)$ varies from negative infinity to positive infinity. To solve this problem, the equivalent capacitance needs to be separated from the equivalent inductance. Hence, another axis needs to be introduced to solve the problem. For the parallel model, the 4th axis is the derivative of voltage (DV). For the series model, the 4th axis is the integral of current (IC).

We can prove that each hyperplane in the 4-D Lissajous coordinates (parallel or series) represents a three-element linear circuit with series or parallel connectivity. For the parallel model, the parallel capacitor can be computed from:

$$C = \frac{N_{DV}}{N_i} \quad (55)$$

where N_{DV} is the DV component of the normal vector \vec{N}_{CF} of the hyperplane in V/s.

According to the 3-D and 4-D Lissajous curve methods described in this section, an equivalent circuit for any nonlinear single-phase circuit (including nonsinusoidal excitation) can be obtained in terms of equivalent energy consumed and stored/restored.

E. Model Selection

Based on a similar approach, the Lissajous method can be applied to obtain a series model. The series model is not developed here because of lack of space.

The parallel model method can identify perfectly any three-element nonlinear parallel system. Meanwhile, the series model method can identify precisely any three-element nonlinear series system. This is irrespective to type of source (current or voltage).

Loads in power systems are connected in parallel and are (intended to be) supplied with voltage excitation; see Fig. 10. Therefore, to obtain active and reactive powers of a black-box, it is wiser to use a parallel circuit (as done by Fryze and Czarnecki).

IV. ILLUSTRATION EXAMPLES

Several examples are discussed in this section to demonstrate the applicability and scopes of the new analytical method. All cases are simulated with the EMTF (Electro-Magnetic Transients Program) [15] and MATLAB to replicate digital data acquisition systems. The voltage source in the first three cases is a cosine function with the following discrete form:

$$v[k] = V_m \cos[\omega k \Delta t] \quad (56)$$

where Δt is the (constant) sampling time. Let us take a voltage amplitude of $\sqrt{2}(120)$ V at a frequency of $f = 50$ Hz, giving a period $T = 20$ ms and $\omega = 100 \pi$ rad/s. The integral of the

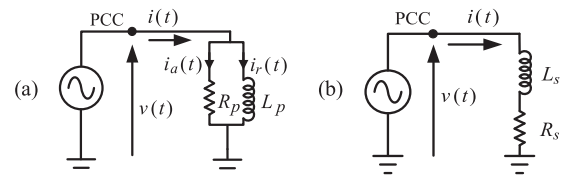


Fig. 11. Topology of the linear circuit: (a) parallel circuit; (b) series circuit.

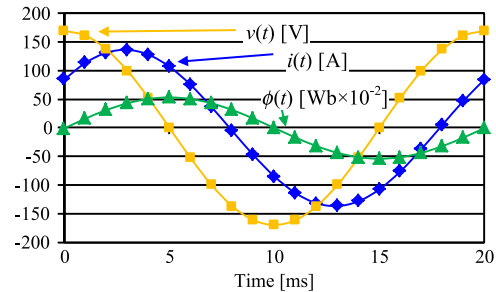


Fig. 12. Numerical data of voltage, current, and flux. The markers in the plot are the 21 points used for calculations.

instantaneous voltage is obtained from a simple discrete integration method (forward Euler) as:

$$\phi[k] = \sum_{i=1}^{i=k} v[i] \Delta t. \quad (57)$$

The instantaneous current derivative DI is computed from the discrete current measured at the terminals as:

$$DI[k] = \frac{di}{dt}[k] = \frac{i[k] - i[k-1]}{\Delta t}. \quad (58)$$

The computation error introduced with (57) and (58) is given by the sampling time. Better numerical methods can be applied of course, but for the sake of illustration let us use (57) and (58).

A. Linear $R - L$ Circuits

The first two examples are the parallel and series $R - L$ linear circuits with $R_p = R_s = 2 \Omega$ and $L_p = L_s = 5$ mH shown in Fig. 11. We start from the knowledge of the instantaneous voltage $v[k]$ and current $i[k]$. To simplify the calculation process, $\Delta t = 1$ ms has been chosen as the sampling time, which means that the number of samples is only 21 (when including the initial and end points). Due to the calculation similarities between the series and parallel models, only the calculations for the parallel circuit are presented, but results for both circuits are provided.

The discretized instantaneous voltage, current, and flux for the parallel circuit are plotted in Fig. 12. To obtain accurate flux data more samplings are needed. Because the voltage source is a cosine function (starts at its peak), therefore, the initial flux for $t = 0$ ($k = 1$) is zero $\phi[1] = 0$.

Assuming that the initial current of the inductor is zero ($k = 0$), the first three points (points 0 to 2) are used to compute the circuit plane; see Fig. 13. Note that, for nonlinear systems, point 0 may not be a point of all linearized circuit planes. Under those conditions one can use points 1 to 3 to calculate the normal vector. For more details see the nonlinear example shown in Fig. 19(b).

According to the numerical results given in Table I, the first normal vector $\vec{N}_{CF}[1] = (-N_v[1], -N_\phi[1], N_i[1])$ can be computed, using point 0, as:

$$\begin{aligned} N_v[1] &= (\phi[2] - 0)(i[1] - 0) - (\phi[1] - 0)(i[2] - 0) = 14.16 \\ N_\phi[1] &= (v[1] - 0)(i[2] - 0) - (i[1] - 0)(v[2] - 0) = 5666 \\ N_i[1] &= (\phi[1] - 0)(v[2] - 0) - (\phi[2] - 0)(v[1] - 0) = 28.33 \end{aligned} \quad (59)$$

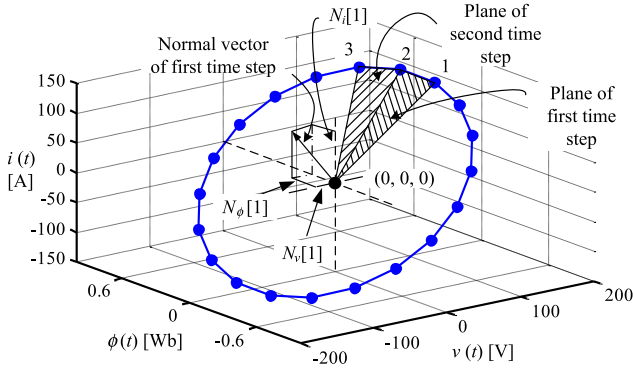


Fig. 13. Detailed computation process for the first and second time steps.

 TABLE I
 DATA FOR THE PARALLEL CIRCUIT

Point (k)	0	1	2	3	4
T [s]	-	0	0.001	0.002	0.003
$v[k]$ [V]	0	169.7056	161.3996	137.2947	99.75047
$\phi[k]$ [Wb]	0	0	0.166928	0.317520	0.437020
$i[k]$ [A]	0	84.85281	114.0854	132.1505	137.2798

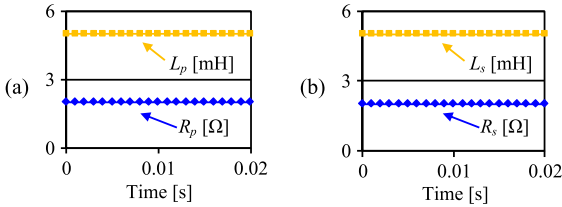


Fig. 14. Calculation results of resistor and inductor: (a) resistor and inductor in parallel circuit; (b) resistor and inductor in series circuit.

where $N_v[1]$ is the amplitude of voltage component of normal vector $\vec{N}_{CP}[1]$, $N_\phi[1]$ is the amplitude of flux component of $\vec{N}_{CP}[1]$, $N_i[1]$ is the current component of $\vec{N}_{CP}[1]$.

Applying (46) and (47) in their discrete form:

$$G_p[k] = \frac{N_v[k]}{N_i[k]} \quad (60)$$

$$L_p^{-1}[k] = \Gamma_P[k] = \frac{N_\phi[k]}{N_i[k]}, \quad (61)$$

we get:

$$R_p^{-1}[1] = G_p[1] = \frac{N_v[1]}{N_i[1]} = \frac{14.16}{28.33} = 0.499[\Omega] \quad (62)$$

and

$$L_p^{-1} = \Gamma_p[1] = \frac{N_\phi[1]}{N_i[1]} = \frac{5666}{28.33} = 200 [\text{H}^{-1}]. \quad (63)$$

Then points 2, 3, and point 0 are used to form a new circuit plane and compute the circuit parameters of the next time period. Repeating this process for all sample points (21 points in this case), the instantaneous parallel resistor and inductor can be obtained; the results are given in Fig. 14(a). One can see that the method identifies correctly the resistance and inductance of the circuit from data (instantaneous voltage and current) obtained at the PCC.

The 3-D series Lissajous curve (3-D SLC) can be applied to compute the circuit parameters of the circuit of Fig. 11(b). One can see from Fig. 14(b) that the resistive and inductive parameters are properly identified.

Once $R(t)$ and $L(t)$ are known, all power quantities can be obtained as described in Section III. The instantaneous active and reactive powers are presented in Fig. 15. The instantaneous

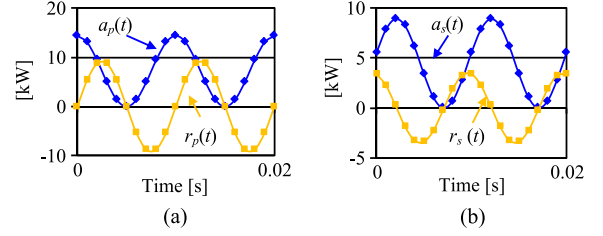
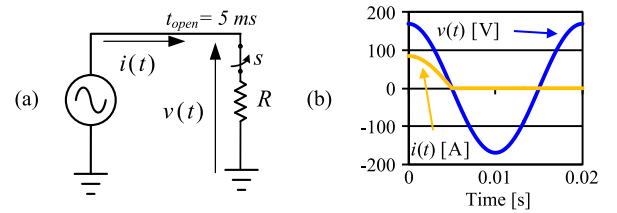

 Fig. 15. Calculation result of active and reactive powers: (a) $a_p(t)$ and $r_p(t)$ for the parallel model; (b) $a_s(t)$ and $r_s(t)$ for the series model.

 TABLE II
 POWER QUANTITIES OF TWO LINEAR CIRCUITS USING ONLY 21 POINTS

	Parallel circuit		Series circuit	
	Computed	Exact	Computed	Exact
P_a [kW]	7.543	7.2	4.729	4.45
P_{re} [kW]	0	0	0.17	0
Q_{textbook} [kvar]	8.72	9.17	3.40	3.50
Q_{1459} [kvar]	8.87	9.17	3.78	3.50
Q_{physical} [kvar]	8.86	9.17	3.71	3.50


 Fig. 16. Circuit of controlled switch with resistor and its terminal measurements: (a) Topology of nonlinear circuit; (b) $v(t)$ and $i(t)$ of the nonlinear circuit.

active power matches with Joule's law and the instantaneous reactive power is equal to the time derivative of the energy stored in the inductor.

The average powers are given in Table II. Note that the results shown in Table II are not very precise because the number of sample points is small. By increasing the samples to 1000 points per cycle, the relative error is reduced to 10^{-4} . For this linear case, the reactive powers of the three expressions discussed in Section III give exactly the same result.

B. Controlled Switch Feeding a Resistor

A simple nonlinear circuit is chosen to illustrate a problem with the IEEE Standard definitions and Czarnecki's CPCs method [16]. In the circuit of Fig. 16, R is in series with a controlled switch s . Assume that the switch opens at $t = 5$ ms (quarter of a cycle) and $R = 2 \Omega$. The time step for this case is chosen as 0.02 ms to reduce the computation error.

By substituting (7) into (17), Q_{1459} can be rewritten as:

$$Q_{1459} = \frac{\omega_1}{kT} \int_{t_0}^{t_0+kT} i_1(t) [\phi_1(t) - \phi_1(t_0)] dt. \quad (64)$$

As discussed in Section III, the factor ω_1 is a coefficient necessary to match the value of classic (textbook) calculation of reactive power. Based on (64), instead of zero reactive power, the reactive power Q_{1459} of a resistive nonlinear circuit is:

$$Q_{1459} = \frac{I_{1m} V_{1m}}{0.04} \int_0^{0.02} \sin(\omega_1 t) \cos(\omega_1 t - \theta_1) dt = 1146.2 [\text{var}] \quad (65)$$

where I_{1m} is the amplitude of $i_1(t)$ (the fundamental current component) and V_{1m} is the amplitude of $v_1(t)$, θ_1 is the angle between $v_1(t)$ and $i_1(t)$. Because Q_{1459} is non-zero it cannot be

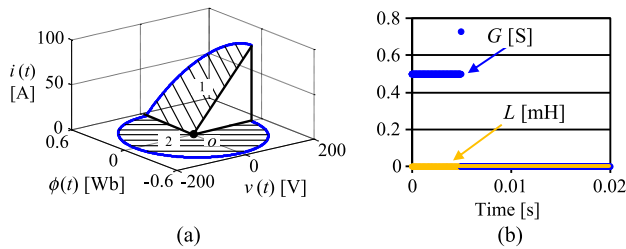


Fig. 17. 3-D Lissajous curve of the nonlinear circuit and the computed parameters: (a) 3-D Lissajous curve in parallel coordinates of nonlinear circuit; (b) $G(t)$ and $L(t)$ computed from 3-D Lissajous curve method. The lines overlap from 0.005 s to 0.02 s.

TABLE III
AVERAGE POWER QUANTITIES OF NONLINEAR CIRCUIT

	Nonlinear Circuit	
	3-D PLC method	Physical definition (Joule's Law)
Average joule power P_a [kW]	1.81	1.8
Average nonlinear loss P_{nz} [kW]	0	0
$Q_{physical}$ [kvar]	0	0

a physically correct reactive power (according to Maxwell equations) since the circuit lacks of elements capable of storing energy. In the following examples we do not calculate Q_{1459} .

The decomposition method CPCs has a similar problem with this nonlinear circuit. The CPCs method computes the load conductance G_{CPCs} of this nonlinear circuit as [4]:

$$G_{CPCs} = \frac{\int_0^T v i dt}{\int_0^T v^2 dt} = \frac{36.14}{288.58} = 0.125 \text{ [S]}. \quad (66)$$

The “active current” i_a through that load conductance G_{CPCs} is:

$$i_a(t) = v(t)G_{CPCs}. \quad (67)$$

This active current is a sinusoidal function in phase with the voltage, is not the current that consumes power in the circuit resistor. It represents the ideal circumstances when the circuit has been fully compensated (for both reactive power and current distortion). In other words, $i_a(t)$ is the current that delivers energy to a linear resistive load that consumes the same active power than the circuit resistor. The reminder current component $i(t) - i_a(t)$ is decomposed into three parts which are “reactive current” $i_r(t)$, “scattered current” $i_s(t)$, and “generated current” $i_g(t)$. The so-called reactive current $i_r(t)$ is

$$i_r(t) = \sqrt{2} \operatorname{Re} \left[\frac{I_{1rms} \sin \theta_1}{j V_{1rms}} V_{1rms} e^{j\omega_1 t} \right] = I_{1m} \sin \theta_1 \sin \omega_1 t \quad (68)$$

where V_{1rms} and I_{1rms} are the rms values of the fundamental components of voltage $v(t)$ and current $i(t)$ measured at the PCC.

Although CPCs method does not claim to be a way to calculate reactive power, modeling a nonlinear circuit as a constant resistor in parallel with three nonlinear elements is not a physically correct identification of this nonlinear circuit. In contrast, the 3-D Lissajous curve method is a comprehensive representation of any parallel circuit under sinusoidal excitation. By applying the proposed process, the correct conductance of this nonlinear circuit can be calculated and the corresponding average and instantaneous powers can be obtained. The results are presented in Fig. 17 and Table III.

According to Fig. 17, the conductance of the circuit is equal to 0.5 S for the first 1/4 of the cycle which is equal to the resistor in the actual circuit. For the following 3/4 of the cycle, the switch opens which causes an open circuit and the computed conductance is zero. The computed zero inductance leads to a zero reactive power at every instant, which satisfies the physical reality

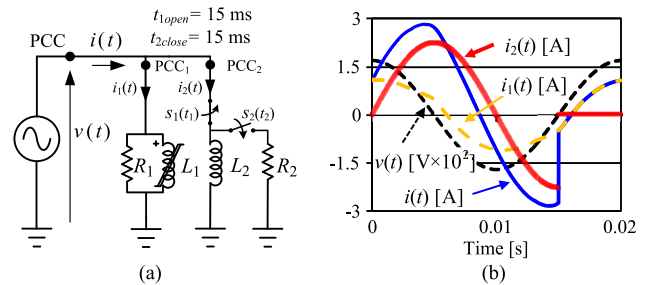


Fig. 18. Topology and measurements of hysteresis and switching nonlinear circuits: (a) topology of hysteresis and switching nonlinear circuit; (b) source voltage $v(t)$ and current of source $i(t)$, current in subsystem 1 $i_1(t)$, current in subsystem 2 $i_2(t)$.

of this nonlinear circuit. Two working states can be clearly seen in the 3-D Lissajous curve of Fig. 17(a), which satisfy the physical states of the switch. The actual active power in a period P_a is:

$$P_a = \frac{1}{0.02} \int_0^{0.02} i^2(t) R dt = 1.8 \text{ [kW]}, \quad (69)$$

and the actual reactive power Q is zero. The comparison between the physical definition, given by Joule's law, and the 3-D PLC method is given in Table III. The power quantities in Table III show that our method is physically correct. Because of (16) cannot be applied to nonlinear circuits, in the remaining examples, $Q_{textbook}$ will not be calculated.

A spike caused by the sudden shift of circuit planes is deliberately shown in Fig. 17(b). This can be easily identified and filtered numerically since the derivative becomes very large at discontinuity points. In the next examples, the spikes are removed by a detection and filtering algorithm.

C. Hysteresis Loss and Nonlinear Loss due to Switching

Two nonlinear energy consumption mechanisms, hysteresis loss and nonlinear consumption due to switching, are discussed in this example. Hysteresis loss is the well-known nonlinear loss in magnetic cores and dielectric materials. Nonlinear energy consumption due to switching appears mainly in power electronic devices when energy is stored in reactive elements and restored to the load (and not returned to the source). The circuit in Fig. 18(a) is designed to illustrate these two phenomena; the terminal measurements are shown in Fig. 18(b). Subsystem 1 is a transformer core in parallel with a linear resistor $R_1 = 200 \Omega$. The hysteresis curve of the transformer core, see Fig. 19(a), is obtained by a nonlinear inductor $L_T(t)$ connected in parallel with a constant resistor $R_T = 740 \Omega$. The behavior of $L_T(t)$ and R_T are shown in Fig. 19(b). Subsystem 2 illustrates the nonlinear energy consumption due to switching. The inductor $L_2 = 240 \text{ mH}$ stores energy from the source in the first 3/4 of the cycle and restores the energy to the linear resistor $R_2 = 200 \Omega$ in the last 1/4 cycle. Resistor R_2 cannot be seen from PCC measurements. Note that many power electronics converters work on the principle of charging and discharging inductors and capacitors; take for example PFC (power factor correction) circuits.

Note that for the nonlinear inductor case shown in Fig. 19(b) the origin (point 0) is not a point of the circuit plane formed by points a and b . By the application of the 3-D Lissajous curve method at the system PCC, subsystem PCC₁, and subsystem PCC₂, the parameters and power quantities of the assembled system and each of the subsystems are obtained

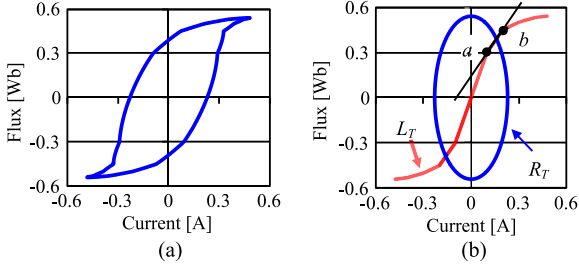


Fig. 19. Generation of transformer core model: (a) Hysteresis loop of transformer core; (b) $\phi - i$ behavior of nonlinear inductor L_T and linear resistor R_T .

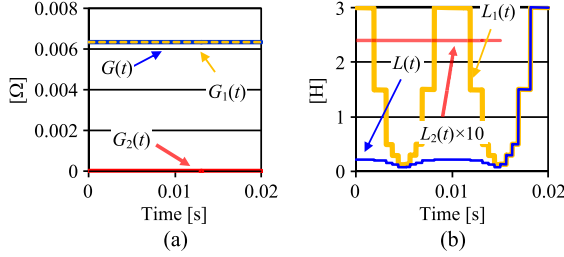


Fig. 20. Computation results of hysteresis and switching nonlinear circuit: (a) equivalent conductance $G(t)$ at PCC, equivalent conductance $G_1(t)$ at PCC₁, and equivalent conductance $G_2(t)$ at PCC₂; $G(t)$ and $G_1(t)$ are overlapped. (b) Inductance $L(t)$ at PCC, inductance $L_1(t)$ at PCC₁, and inductance $L_2(t)$ at PCC₂; $L(t)$ and $L_1(t)$ are overlapped when s_1 is open from 0.015 s to 0.02 s.

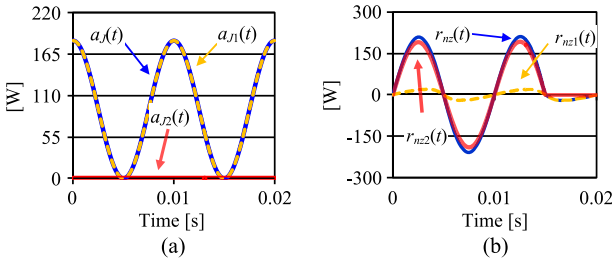


Fig. 21. Power quantities of each subsystem and system: (a) instantaneous joule power $a_J(t)$ of the system, instantaneous joule power $a_{J1}(t)$ of subsystem 1, and instantaneous joule power $a_{J2}(t)$ of subsystem 2; $a_J(t)$ and $a_{J1}(t)$ are overlapped. (b) Instantaneous power $r_{nz}(t)$ of the system, instantaneous power $r_{nz1}(t)$ of subsystem 1, and instantaneous power $r_{nz2}(t)$ of subsystem 2.

as shown in Figs. 20 and 21. Instead of calculating a constant resistor R_1 , $G_1(t)$ is equal to the conductance of R_1 in parallel with the hysteresis loss in R_T . In other words, from the measurements at PCC₁, the hysteresis loss of the transformer core cannot be distinguished from the joule loss in R_1 . Hence, $L_1(t)$ equals $L_T(t)$. The conductance of subsystem 2, shown in Fig. 20(a), is zero at all times which satisfies the fact that R_2 cannot be seen at PCC₂. The inductances in Fig. 20(b) are calculated based on (50). A clear switching action can be seen in Fig. 20(b) at 15 ms, which produces nonlinear energy consumption. According to Fig. 21(b), the nonlinear consumption due to switching is acting as an incomplete reactive power $r_{nz2}(t)$ (lacks one quarter of the restoring process). Based on the physical definition of consumed power, we can calculate the total consumed power P_C in one period as:

$$P_C = \frac{1}{T} \int_0^T v(t)i(t)dt \stackrel{T \rightarrow 0.02}{=} 122 \text{ [W]}. \quad (70)$$

TABLE IV
AVERAGE POWER QUANTITIES OF HYSTERESIS AND SWITCHING NONLINEAR CIRCUIT

Nonlinear Circuit	Source	Subsystem 1	Subsystem 2
Average joule power P_a [W]	90.9	90.9	0
Average nonlinear loss P_{nz} [W]	31.1	0	31.1
$Q_{physical}$ [var]	117	20.8	96.6

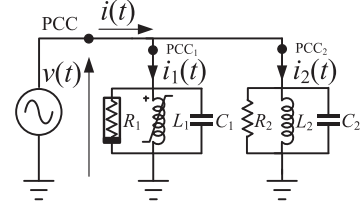


Fig. 22. Topology of nonlinear circuit with nonsinusoidal excitation.

After obtaining the correct circuit parameters, the power quantities can be easily calculated as shown in Table IV. By comparing the results shown in Table IV with P_C , we conclude that:

$$P_C = P_a + P_{nz} \quad (71)$$

which means that the calculations are correct.

Based on the simulation parameters, the power in R_1 and R_T can be obtained from Joule's Law as (see (20)):

$$\begin{aligned} P_{R_1+R_T} &= \frac{1}{T} \int_0^T \left(\frac{v^2(t)}{R_1} + \frac{v^2(t)}{R_T} \right) dt = \frac{V_m^2}{2R_1} + \frac{V_m^2}{2R_T} \\ &= 91.4 \text{ [W]} \\ &\approx P_a \end{aligned} \quad (72)$$

which is nearly equal to the result shown in Table IV.

The 3-D Lissajous method also provides a new view of reactive power. The part of the instantaneous power of the inductor that is restored to the source is reactive power. The part of the instantaneous power of the inductor that is eventually consumed becomes active power. The reactive power Q_{L_2} of the inductor L_2 can be calculated analytically as:

$$\begin{aligned} Q_{L_2} &= \frac{\pi}{2T} \int_0^{\frac{T}{2}} |r_{L_2}(t)| dt = \frac{V_m^2}{4\omega L_2} = 95.49 \text{ [var]} \\ &\approx Q_{physical}(\text{Subsystem 2}) \end{aligned} \quad (73)$$

which means 3-D Lissajous method has a correct physical meaning in Maxwell terms.

D. Circuit with Nonsinusoidal Voltage Excitation

To verify the 4-D Lissajous curve method and the additivity of the power quantities obtained by the Lissajous curve method for the parallel model, a circuit with two subsystems is introduced in Fig. 22. In this nonlinear circuit, R_1 and L_1 are nonlinear elements with behavior shown in Fig. 23. R_2 and L_2 are linear elements where $R_2 = 1 \Omega$ and $L_2 = 10 \text{ mH}$. C_1 and C_2 are linear capacitors, where $C_1 = 0.1 \text{ mF}$ and $C_2 = 1 \text{ mF}$. A voltage source containing fundamental component, 2nd and 3rd harmonics is selected for this case. The discrete voltage function of this source, with $V_m = 120\sqrt{2} \text{ V}$ and $\omega = 100 \pi \text{ rad/s}$, is:

$$v[k] = V_m \cos[\omega k \Delta t] + \frac{V_m}{2} \cos \left[2\omega k \Delta t + \frac{\pi}{6} \right] + \frac{V_m}{3} \cos \left[3\omega k \Delta t + \frac{\pi}{3} \right]. \quad (74)$$

By the application of the method described in this paper to each subsystem and system separately, the parameters of each

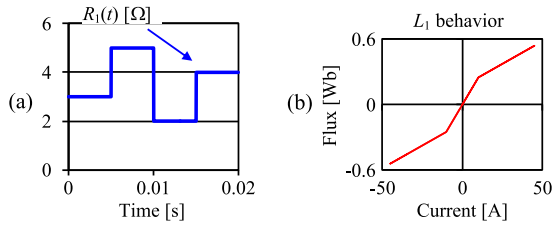


Fig. 23. Behavior of nonlinear elements in the nonlinear circuit: (a) nonlinear behavior of resistor; (b) nonlinear behavior of inductor.

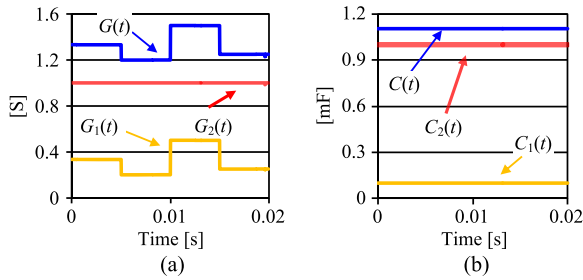


Fig. 24. Computation results of the nonlinear circuit: (a) Equivalent conductance $G(t)$ at PCC, equivalent conductance $G_1(t)$ at PCC₁, and equivalent conductance $G_2(t)$ at PCC₂; (b) equivalent capacitance $C(t)$ at PCC, equivalent capacitance $C_1(t)$ at PCC₁, and equivalent capacitance $C_2(t)$ at PCC₂.

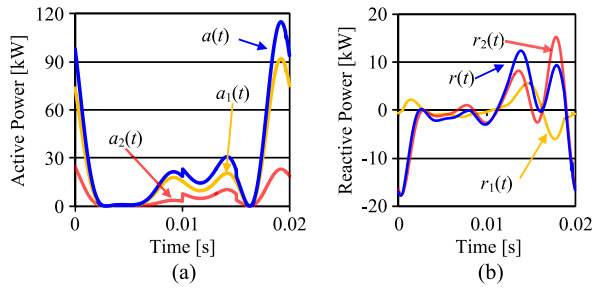


Fig. 25. Active power and reactive power of each subsystem and system: (a) active power $a(t)$ of the system, active power $a_1(t)$ of subsystem 1, and active power $a_2(t)$ of subsystem 2; (b) reactive power $r(t)$ of the system, reactive power $r_1(t)$ of subsystem 1, and reactive power $r_2(t)$ of subsystem 2.

TABLE V
AVERAGE POWER QUANTITIES OF NONLINEAR CIRCUIT

Nonlinear Circuit	Source	Subsystem 1	Subsystem 2
Average joule power P_e [kW]	25.4	5.92	19.5
Average nonlinear loss P_{nz} [kW]	0.07	0.005	0.07
$Q_{physical}$ [kvar]	7.18	2.88	6.97
Q_C [kvar] (physical)	10.4	0.95	9.46
Q_L [kvar] (physical)	8.93	3.58	5.34

subsystem and the total system can be obtained accurately. The results are shown in Figs. 24 and 25, and in Table V. Based on the correct resistances and capacitances computed from (46) and (55) respectively, the inductances can be obtained based on KCL and (50).

According to Fig. 24(a), the equivalent conductances perfectly match the parameters used in the simulation, where $G_1(t)$ equals $R_1^{-1}(t)$ and $G_2(t)$ is the conductance ($R_2^{-1}(t)$) of the parallel equivalent circuit of subsystem 2. The additivity of conductances is then confirmed:

$$G(t) = G_1(t) + G_2(t). \quad (75)$$

The additivity can also be found in capacitance where $C_1(t)$ plus $C_2(t)$ equals to $C(t)$, see Fig. 24(b). Because the conductances

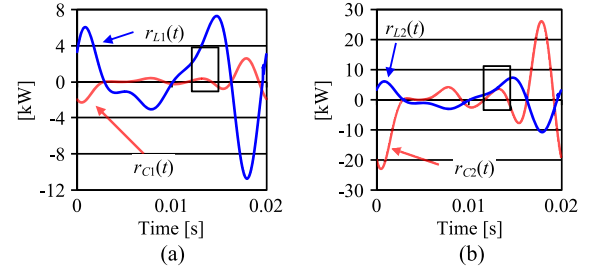


Fig. 26. Instantaneous power of capacitor and inductor in each subsystem. (a) Instantaneous power $r_{L1}(t)$ of $L_1(t)$ and instantaneous power $r_{C1}(t)$ of $C_1(t)$; (b) instantaneous power $r_{L2}(t)$ of $L_2(t)$ and instantaneous power $r_{C2}(t)$ of $C_2(t)$. One can see that for nonsinusoidal excitation inductors and capacitors can store and restore energy at the same time.

can be properly added, the instantaneous power quantities can also be added:

$$a(t) = a_1(t) + a_2(t) \quad (76)$$

$$r(t) = r_1(t) + r_2(t). \quad (77)$$

One can see from Table V that the average active powers P_o can be added.

The reactive power compensation between the two subsystems can be observed from Fig. 25(b). As one can see, the reactive compensation becomes complicated for nonsinusoidal excitation. From Fig. 26 one can see that there are regions where inductive and capacitive instantaneous reactive powers have opposite signs and thus partially compensate each other, but there are other regions where they add. Thus, under nonsinusoidal excitation, different from sinusoidal excitation, the capacitor and inductor can store energy at the same time; see the regions in boxes in Fig. 26.

Because the absolute value calculation is a nonlinear operation, $Q_{physical}$ is not equal to the difference of the reactive power Q_L (equivalent inductor) and the reactive power Q_C (equivalent capacitor) in each subsystem. Mathematically, we have:

$$\begin{aligned} Q_{physical} &= \frac{\pi}{2T} \int_0^T |v(t)i_L(t) + v(t)i_C(t)| dt \\ &\neq \frac{\pi}{2T} \int_0^T |v(t)i_L(t)| dt - \frac{\pi}{2T} \int_0^T |v(t)i_C(t)| dt \\ &\neq Q_L - Q_C. \end{aligned} \quad (78)$$

Consequently, $Q_{physical}$ of the system is not equal to the summation of $Q_{physical}$ in each subsystem; see Table V.

Due to the properties of the 4-D Lissajous curve tool, separating $Q_{physical}$ into capacitive reactive power Q_C and inductive reactive power Q_L in Table V is a wiser choice because they add: $Q_C = 0.95 + 9.46 = 10.4$ kvar and $Q_L = 3.58 + 5.34 = 8.93$ kvar. Inductive, or capacitive, reactive power can be added independently, but $Q_{physical}$ does not have this property for nonsinusoidal voltage excitation.

V. CONCLUSION

A graphical-analytical tool has been presented for the calculation of the instantaneous active and reactive powers in nonlinear circuits from only terminal measurements. The tool has full physical meaning since it is derived from the Poynting Vector Theorem.

The method first identifies the circuit components, $R(t)$, $L(t)$, and $C(t)$ of the nonlinear system model (series or parallel). Then the instantaneous active $a(t)$ and reactive $r(t)$ powers are computed from basic electromagnetic principles. Last, the average powers, P and Q , are computed from integration of the instantaneous energy consumed and the energy that is stored and restored based on Maxwell theory.

Four examples illustrate the application and virtues of the identification method proposed in the paper.

This paper closes the theoretical gap in the power theory for non-linear circuits by providing a physically consistent definition (in Maxwell terms) and a computation method for reactive power.

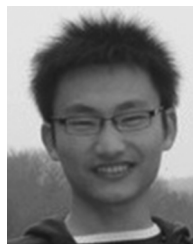
ACKNOWLEDGMENT

The authors would like to thank Dr. Julien Sandraz for interesting discussions at the early stages of this research. The second author would like to thank Dr. José Cohen for the many years of discussions on the physical meaning of power. Last, but not least, the authors would also like to recognize the meticulous review of our paper and valuable comments by the reviewers and in particular Reviewer 1.

REFERENCES

- [1] C. P. Steinmetz, *Theory and Calculation of Alternating Current Phenomena*, 1st ed. New York: McGraw-Hill, 1897.
- [2] *IEEE Standard Definitions for the Measurement of Electric Power Quantities under Sinusoidal, Nonsinusoidal, Balanced, or Unbalanced Conditions*, IEEE Std. 1459-2010, 2010, 1–40.
- [3] L. S. Czarnecki, “Budeanu and Fryze: Two frameworks for interpreting power properties of circuits with nonsinusoidal voltages and currents,” *Electr. Eng.*, vol. 80, pp. 359–367, Dec. 1997.
- [4] L. S. Czarnecki, “An orthogonal decomposition of the current of nonsinusoidal voltage source applied to nonlinear loads,” *Int. J. Circuit Theory Appl.*, vol. II, pp. 235–239, 1983.
- [5] L. S. Czarnecki, “Orthogonal decomposition of the current in a three-phase nonlinear asymmetrical circuit with nonsinusoidal voltage,” *IEEE Trans. Instrum. Meas.*, vol. IM-37, no. 1, pp. 30–34, Mar. 1988.
- [6] F. de León and J. Cohen, “Discussion of ‘Instantaneous reactive power p-q theory and power properties of three-phase systems’,” *IEEE Trans. Power Del.*, vol. 23, pp. 1693–1694, Jul. 2008.
- [7] A. E. Emanuel, “Powers in nonsinusoidal situations—A review of definitions and physical meaning,” *IEEE Trans. Power Del.*, vol. 5, pp. 1377–1389, Jul. 1990.
- [8] A. E. Emanuel, “Poynting vector and the physical meaning of non-active powers,” *IEEE Trans. Instrum. Meas.*, vol. 54, pp. 1457–1462, May 2005.

- [9] P. E. Sutherland, “On the definition of power in an electrical system,” *IEEE Trans. Power Del.*, vol. 22, pp. 1100–1107, Apr. 2007.
- [10] L. S. Czarnecki, “Could power properties of three-phase systems be described in terms of the Poynting vector?,” *IEEE Trans. Power Del.*, vol. 21, pp. 339–344, Jan. 2006.
- [11] F. de León and J. Cohen, “AC power theory from Poynting theorem: Accurate identification of instantaneous power components in nonlinear-switched circuits,” *IEEE Trans. Power Del.*, vol. 25, pp. 2104–2112, Oct. 2010.
- [12] F. de León, L. Qaseer, and J. Cohen, “AC power theory from Poynting theorem: Identification of the power components of magnetic saturating and hysteretic circuits,” *IEEE Trans. Power Del.*, vol. 27, pp. 1548–1556, Jul. 2012.
- [13] M. S. Erlicki and A. Emanuel, “New aspects of power factor improvements part I—Theoretical basis,” *IEEE Trans. Ind. Gen. Appl.*, vol. IGA-4, pp. 441–446, Jul. 1968.
- [14] J. W. Nilsson and S. A. Riedel, *Electric Circuits*, 6th ed. Upper Saddle River, NJ, USA: Prentice-Hall, 2000.
- [15] DCG-EMTP (Development coordination group of EMTP) Version EMTP-RV, Electromagnetic Transients Program [Online]. Available: <http://www.emtp.com>
- [16] M. Castro-Nunez and R. Castro-Puche, “The IEEE standard 1459, the CPC power theory, geometric algebra in circuits with nonsinusoidal sources and linear loads,” *IEEE Trans. Circuits Syst. I, Reg. Papers*, vol. 59, no. 12, pp. 2980–2990, Dec. 2012.



Tianqi Hong (S'13) was born in Nanjing, China, in 1989. He received the B.Sc. degree in electrical engineering from Hohai University, China, in 2011, and the M.Sc. degree in the same field from Southeast University, China, and the Electrical and Computer Engineering Department, New York University (NYU), New York, respectively. He is currently a Ph.D. candidate in the Polytechnic School of Engineering, NYU. His main interests are electromagnetic design and power systems.



Francisco de León (S'86–M'92–SM'02–F'15) received the B.Sc. and the M.Sc. (Hons.) degrees in electrical engineering from the National Polytechnic Institute, Mexico City, Mexico, in 1983 and 1986, respectively, and the Ph.D. degree in electrical engineering from the University of Toronto, Toronto, ON, Canada, in 1992.

He has held several academic positions in Mexico and has worked for the Canadian electric industry. Currently, he is an Associate Professor with the Department of Electrical and Computer Engineering at New York University, New York. His research interests include the analysis of power phenomena under nonsinusoidal conditions, the transient and steady-state analyses of power systems, the thermal rating of cables and transformers, and the calculation of electromagnetic fields applied to machine design and modeling.

Prof. de León is an Editor of the IEEE TRANSACTIONS ON POWER DELIVERY and the IEEE *Power Engineering Letters*.